Electrochemical and thermal characterization of doped ceria electrolyte with lanthanum and zirconium

Rafique, Asia; Raza, Rizwan; Arifin, Nor; Ullah, M. Kaleem; Ali, Amjad; Steinberger-Wilckens, Robert

DOI:
10.1016/j.ceramint.2018.01.048

Document Version
Peer reviewed version

Citation for published version (Harvard):
Rafique, A, Raza, R, Arifin, N, Ullah, MK, Ali, A & Steinberger-Wilckens, R 2018, 'Electrochemical and thermal characterization of doped ceria electrolyte with lanthanum and zirconium', *Ceramics International*, vol. 44, no. 6, pp. 6493-6499. https://doi.org/10.1016/j.ceramint.2018.01.048

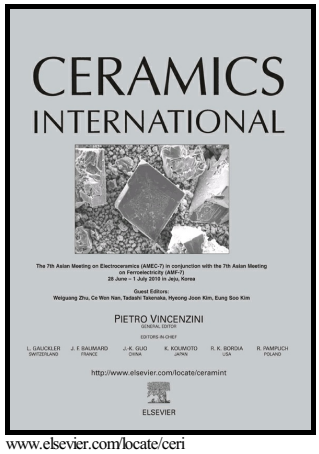

www.elsevier.com/locate/ceri

Electrochemical and Thermal Characterization of Doped Ceria Electrolyte with Lanthanum and Zirconium

Asia Rafique, Rizwan Raza, Nor Anisa Arifin, M Kaleem Ullah, Amjad Ali, Robert Steinberger-Wilckens

PII: S0272-8842(18)30060-9
DOI: https://doi.org/10.1016/j.ceramint.2018.01.048
Reference: CERI17180

To appear in: *Ceramics International*

Received date: 21 December 2017
Revised date: 5 January 2018
Accepted date: 7 January 2018

Cite this article as: Asia Rafique, Rizwan Raza, Nor Anisa Arifin, M Kaleem Ullah, Amjad Ali and Robert Steinberger-Wilckens, Electrochemical and Thermal Characterization of Doped Ceria Electrolyte with Lanthanum and Zirconium, *Ceramics International,* https://doi.org/10.1016/j.ceramint.2018.01.048

Electrochemical and Thermal Characterization of Doped Ceria Electrolyte with Lanthanum and Zirconium

Asia Rafique[1,2,3], Rizwan Raza[1], Nor Anisa Arifin[3], M Kaleem Ullah[1], Amjad Ali[1], Robert Steinberger-Wilckens[3]

[1]Department of Physics, COMSATS Institute of Information Technology, Lahore 54000, Pakistan

[2] Higher Education Department, Govt. of Punjab, Lahore, 54000, Punjab, Pakistan

[3]Centre for Hydrogen and Fuel Cell Research, School of Chemical Engineering, University of Birmingham, Edgbaston, Birmingham, B15 2TT, UK

Abstract

Nanocomposites electrolytes consisting of La^{3+} and Zr^{4+} doped with ceria labelled as $La_{0.2}Ce_{0.8}O_{2-\delta}$ (LDC), $Zr_{0.2}Ce_{0.8}O_{2-\delta}$ (ZDC) and $Zr_{0.2}La_{0.2}Ce_{0.6}O_{2-\delta}$ (ZLDC) have been synthesized via a co-precipitation route. DC conductivity was studied with a four-probe method in the range of temperature 450 to 650 ˚C and maximum conductivity was found to be 0.81×10^{-2} $S.cm^{-1}$ (LDC) > 0.311×10^{-2} $S.cm^{-1}$ (ZLDC) > 0.15×10^{-2} $S.cm^{-1}$ (ZDC) at a temperature of 650 °C, respectively. Further, electric behavior of doped and co-doped ceria electrolytes was investigated by A.C electrochemical impedance spectroscopy (frequency range ~ 0.1Hz− 4MHz). The phase/structural identification of the material prepared was studied using X-ray diffraction and found ceria to possess a cubic fluorite structure. Scanning electron microscopy (SEM) was carried out to study its morphology and particle size (~ 90-120 nm). Thermal behavior on its change in weight and length with the temperature were studied by thermogravimetric analysis (TGA) and dilatometry respectively. Furthermore, thermal expansion coefficients (TECs) of prepared electrolytes are calculated and found as follows: 13.4×10^{-6} $^oC^{-1}$, 13.6×10^{-6} $^oC^{-1}$and 15.3×10^{-6} $^oC^{-1}$ for LDC, ZDC and ZLDC, respectively, in the temperature range 150− 1150 ^oC.

Keywords: Doped ceria, Co-doped ceria, Electrolyte, Lanthanum, Zirconium, Ionic conductivity, Thermal expansion coefficient.

Introduction

Solid oxide fuel cells (SOFCs) are one of the most promising energy conversion devices due to fascinating features such as: excellent efficiency, low emission and fuel flexibility [1-3]. Yttria stabilized zirconia (YSZ) is the most common electrolyte used in SOFCs because of its good ionic conductivity and stability under both reducing and oxidizing atmosphere [4-5]. But its high operating temperature range 800-1000 °C causes certain limitation; for instance, it blocks the ion migration at the cathode-electrolyte interface by generating insulating phases with lanthanum and strontium based cathodes [6]. Scandia stabilized zirconia has shown good conductivity, but it encounters thermal expansion mismatch problems at high temperature Yb_2O_3, Bi_2O_3, Al_2O_3 or Ga_2O_3 with ScSZ [10-15] and also for a particular composition such as for scandia (10 mol%) and ceria (1 mol%) co-doped zirconia [10]. Therefore, such restraints put interest and need to develop new promising electrolyte materials for low-temperature SOFC (LT-SOFC) e.g., salt oxide composites materials and nanocomposites for advanced fuel cell [16-17]. The well-known solid electrolyte materials; MO_2 (M= Zr, Ce) are still prominent candidates for SOFCs [18]. Doped ceria exhibits good ionic conductivity as compared to stabilized zirconia by generating oxygen vacancies through which oxygen ions easily conduct [19-23]. Ceria doping/co-doping is a good approach to increase the ionic oxide conductivity by structural modification of CeO_2 [24], however there is the downside of ceria-based electrolytes as the electronic conductivity increases under lower oxygen partial pressure ($< 10^{-10}$ atm) due to reduction of Ce^{4+} into Ce^{3+} [25]. Therefore, many researchers have to date reported various rare-earth metal ions and transition elements such as La^{3+}, Dy^{3+}, Gd^{3+}, Sm^{3+}, Eu^{3+}, Nd^{3+}, Y^{3+}, Er^{3+}, Ca^{2+}, Sr^{2+} to enhance the ionic conductivity of ceria based electrolytes [26-29]. The improvement in ionic conductivity of doped ceria is due to an increase of oxygen vacancies. However, these vacancies are not free but are associated with dopant cations and may be ascribed to defect association or clustering of oxygen vacancies after reaching maximum dopant concentration [30]. Ionic conductivity is also influenced by valence and ionic radii of dopant cations. Compatibility between ionic radii of the host cation (Ce^{4+}) and dopant is significant to get the desired lattice strain, otherwise mismatching introduces large lattice strain and hence ionic conductivity tends to decrease [31]. Moreover, the binding energy of the dopant lattice must be low to increase oxygen vacancies [31]. Furthermore, ceria based electrolytes possess weak mechanical strength and may go through mechanical and thermal stress during cell fabrication and high temperature operation

which confines its realization in practical applications [32, 33]. Hence, ceria mechanical strength can be slightly improved with the addition of rare-earth oxides because an increase in oxygen vacancies contributes to weaken the binding energy which results in the increase in thermal expansion coefficient (TEC) [34]. Therefore, the TEC of constituent components of an SOFC must match to prevent cracking during thermal cycling and thus lead to more stability of the FC in transient operation [35,36].

This present work focuses on the development of doped/co-doped ceria electrolytes with lanthanum and zirconium to study their electrochemical and thermal characteristics. For this, $La_{0.2}Ce_{0.8}O_{2-\delta}$ (LDC28), $Zr_{0.2}Ce_{0.8}O_{2-\delta}$ (ZDC28) and $Zr_{0.2}La_{0.2}Ce_{0.6}O_{2-\delta}$ (ZLDC226) were synthesized with co-precipitation method for LT-SOFCs. The morphology and crystal structure of these nanocomposite electrolytes were studied by X-ray diffraction (XRD) and scanning electron microscopy (SEM). Thermal behavior with respect to its weight and length with change in temperature was studied by thermogravimetric analysis (TGA) and dilatometry respectively. Thermal analysis was performed to calculate thermal expansion coefficients (TECs) of these ceria electrolytes in different temperature ranges from room temperature (RT) to 1450 °C. The DC conductivity was determined with a four-probe method in the temperature range 450 to 650 °C in air and electrochemical impedance analysis (EIS) was studied for these ceria electrolytes.

Experimental

Synthesis of Ceria Doped Electrolytes

The samples or nanocomposites for ceria doping $La_{0.2}Ce_{0.8}O_{2-\delta}$ and $Zr_{0.2}Ce_{0.8}O_{2-\delta}$ were labelled LDC and ZDC, respectively, while the sample for ceria co-doping $Zr_{0.2}La_{0.2}Ce_{0.6}O_{2-\delta}$ was labelled ZLDC. These three samples were synthesized via a co-precipitation route [37]. All chemicals: cerium nitrate hexahydrate $Ce(NO_3)_3.6H_2O$, lanthanum nitrate hexahydrate $La(NO_3)_3.6H_2O$, zirconium nitrate pentahydrate $Zr(NO_3)_4.5H_2O$ and sodium carbonate Na_2CO_3 were purchased from Sigma Aldrich (99.9%). For the synthesis of LDC and ZDC powders, the mol% ratio between ceria and lanthanum/zirconium was kept as 4:1 and for co-doped ceria ZLDC, the mol% ratio of ceria, lanthanum and zirconium was considered as 3:1:1. Aqueous solutions of nitrates from the stoichiometric amount of cerium nitrate and lanthanum nitrate/zirconium nitrate were prepared to make 0.1 M solution and were stirred and heated at 80

°C on a hot plate. Another aqueous solution of sodium carbonate with 0.2 M was prepared and added to the nitrate solution dropwise to keep the PH of the solution maintained at 10. The resultant solution was further stirred 1 to 2 hours until a precipitant formed which was rinsed with de-ionized water to remove nitrates, followed by vacuum filtering. The precipitate was kept in an oven for drying at 200 °C for two hours, sintered in a furnace at 900 °C for four hours and afterward well ground to receive the electrolyte powder.

Microstructure Characterization and Thermal Analysis

The sintered powders $La_{0.2}Ce_{0.8}O_{2-\delta}$ (LDC), $Zr_{0.2}Ce_{0.8}O_{2-\delta}$ (ZDC) and $Zr_{0.2}La_{0.2}Ce_{0.6}O_{2-\delta}$ (ZLDC) were characterized by x-ray diffractometery (PANalyticalX'Pert Pro MPD, Netherlands) using monochromated Cu Kα radiation with wavelength λ = 0.15418 nm. The lattice constant and lattice parameter were calculated from their XRD peaks. The average crystallite size "D" was determined by using this Scherrer formula:

$$D = \frac{k\lambda}{\beta \cos \theta} \qquad \text{(i)}$$

Where the Scherrer constant "k" (shape factor) has a value between 0.89 (spherical particles) and 0.94 (cubic particle); it is 0.9 for unknown shaped particles as in this work, "β" is the corrected full width at half maxima (FWHM) of peak, "θ" is the Bragg angle and "λ" is the wavelength of radiation.

The microstructure of the electrolyte samples was analyzed by scanning electron microscopy (FEI Nova NanoSEM 450). The thermal behavior of the composites was investigated by thermogravimetry analysis (TGA) (model Q600, USA) and dilatometry (DIL 402 C, NETZSCH). TGA was carried out to investigate the weight change with increase in temperature using a gas flow of 20 ml/min in nitrogen atmosphere. The linear thermal expansion measurements were carried out with dilatometry from room temperature to 1450 °C using a heating and cooling rate of 20 °C/min. TECs "α" of the samples were calculated by using below formula:

$$\alpha = \frac{dL}{Lo} \times \frac{1}{dT} \qquad \text{(ii)}$$

Where dL= difference of initial and final lengths, L_o = initial length and dT = difference of final and starting temperature.

D.C Conductivity and A.C Electrochemical Impedance Spectroscopy (EIS)

For the measurement of both D.C conductivity and EIS, pellets with dimensions: diameter 1.3 cm and thickness 0.2 cm were fabricated from the three electrolyte powders LDC, ZDC and ZLDC. Then pellets were sintered at 700 °C for one hour and silver paste was coated on both sides of the pellet and dried well to get solid silver electrodes on both sides of the electrolyte. The D.C conductivity of these electrolyte was determined with a four-probe method using a Keithley source meter 2450 SMU in the temperature range 450 to 650 °C in air.

The electrical behavior of these ceria based electrolytes was investigated by A.C electrochemical impedance spectroscopy using a PARSTAT 4000 (Princeton Applied Research, USA) in air with the frequency range ~ of 0.1Hz to 4MHz. The impedance data was simulated with software ZSimpWin, and equivalent circuits were drawn.

Results and Discussion:

Phase and microstructural analysis

XRD analysis of prepared electrolytes LDC, ZDC and ZLDC is shown in Figure. 1 in dependence of 2θ (in the range from 20° to 90°). All sharp peaks of the sintered powder are ceria peaks card no. [96-900-9009] corresponding to the indices (111), (200), (220), (311), (222), (400), (331), (420) and (422) with cubic fluorite structure. No peaks of La and Zr are seen on the XRD pattern which shows that both La and Zr are completely doped in Ce; this also shows the absence of any other diffraction peak of crystalline impurities. Only a slight shifting of 2θ towards smaller/larger angles is observed which leads to the change in lattice parameter of doped electrolytes. This change is due to the difference in the ionic radii of La^{3+} (1.15 Å) and Zr^{4+} (0.86 Å) with Ce^{4+} (0.97 Å) which results in the slight increase in the lattice strain/microstrain [38]. For sample LDC, peaks are slightly shifted toward smaller angles as La^{3+} ionic radius is larger than Ce^{4+}, while peaks are shifted toward larger angles for sample ZDC. For ZLDC, peak shifting is not prominent except some higher angles peaks are slightly shifted toward smaller 2θ.

This strain is good for helping in the improvement of ionic conductivity of ceria doped and co-doped electrolyte as compared to pure ceria electrolytes. The possible cause of microstrain is the

deficiency of oxygen or oxygen vacancies due to the substitution of larger or smaller ionic radii at the site of Ce^{4+}. For smaller 2θ, peaks are sharper which corresponds to larger crystallite size but as 2θ shifts to higher angles, the peaks become wider which corresponds to smaller crystallite size. Lattice parameters "a" and crystallite size "D" for each electrolyte were calculated from the peaks and are shown in Table.1. It shows that the lattice parameter of ZDC is smaller than for the other samples and its peak is shifted to larger angles because the ionic radius of Zr^{4+} is smaller compared to Ce^{4+}.

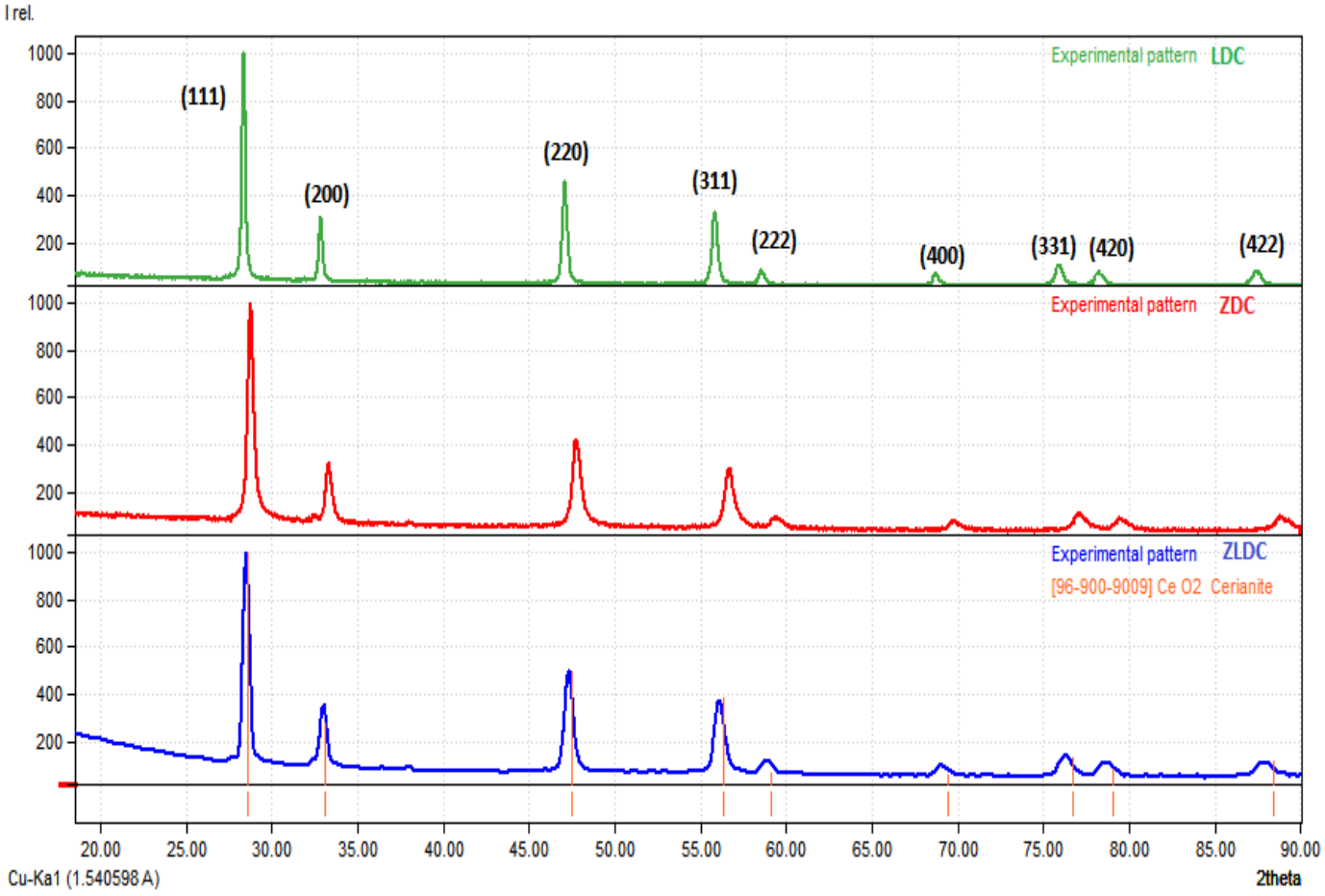

Figure 1: XRD pattern of $La_{0.2}Ce_{0.8}O_{2-\delta}$ (LDC), $Zr_{0.2}Ce_{0.8}O_{2-\delta}$ (ZDC) and $Zr_{0.2}La_{0.2}Ce_{0.6}O_{2-\delta}$ (ZLDC).

Table. 1: Lattice parameter, crystallite size and activation energy of LDC, ZDC and ZLDC

Electrolyte	Lattice Parameter 'a' (Å)	Crystallite Size 'D' (nm)	Activation Energy, E_a (eV)
LDC	5.46	43	0.86
ZDC	5.39	44	0.88
ZLDC	5.43	21	0.87

The morphologies of the compositions LDC, ZDC and ZLDC were observed and analyzed by SEM and typical micrographs of these synthesized powders are shown in Figure 2. The images depict that these nanoparticles of nearly uniform size are well dispersed with dense structure with no apparent porosity. It also reveals that the nanocomposites consist of fine particles of size in the range of 90- 120 nm which is larger than the crystallite size (20-45nm). Hence, particle size is large enough to consist of more than two crystallites.

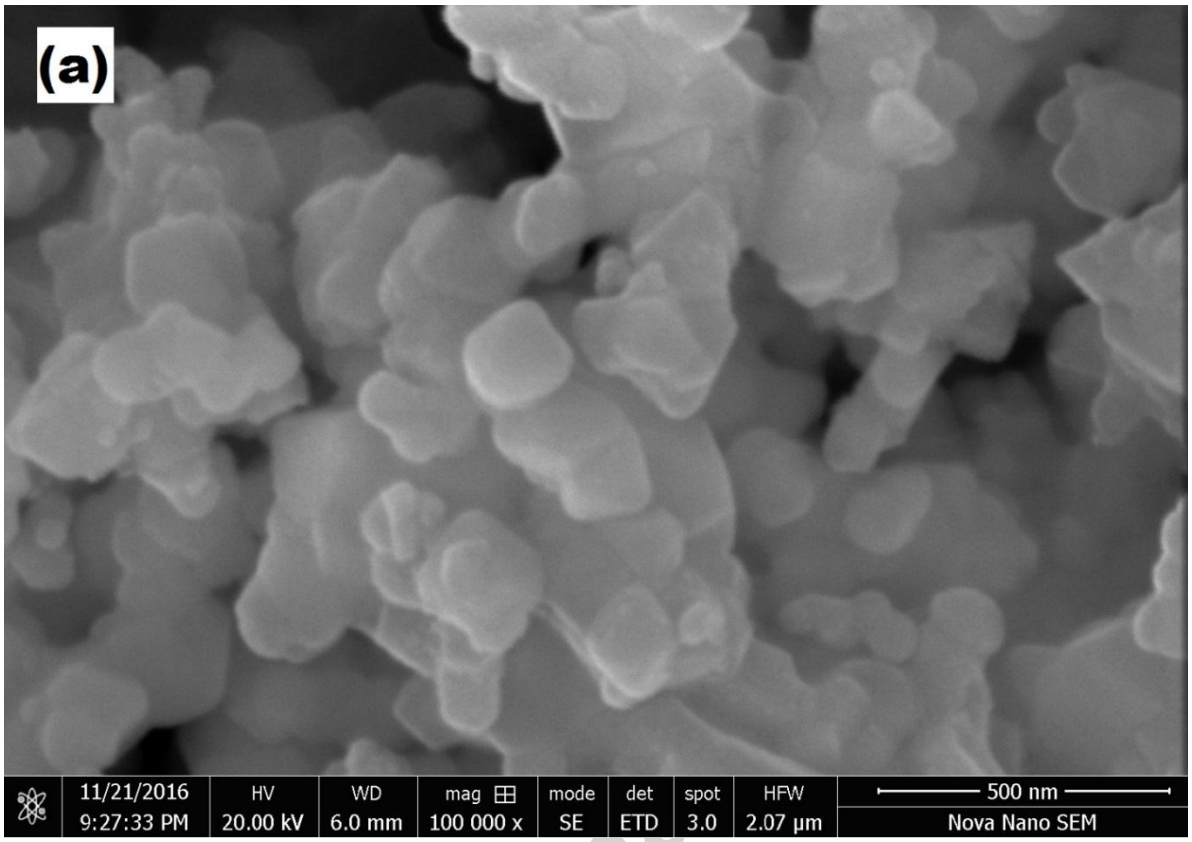

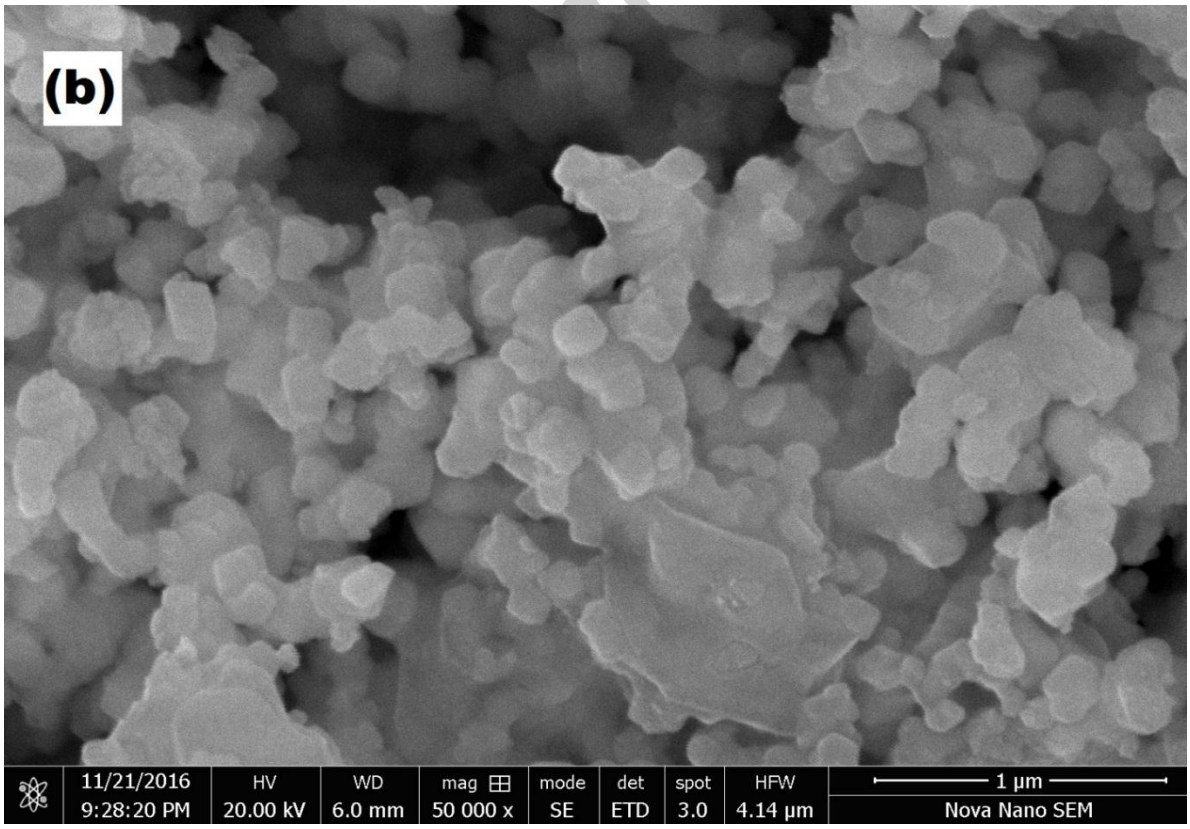

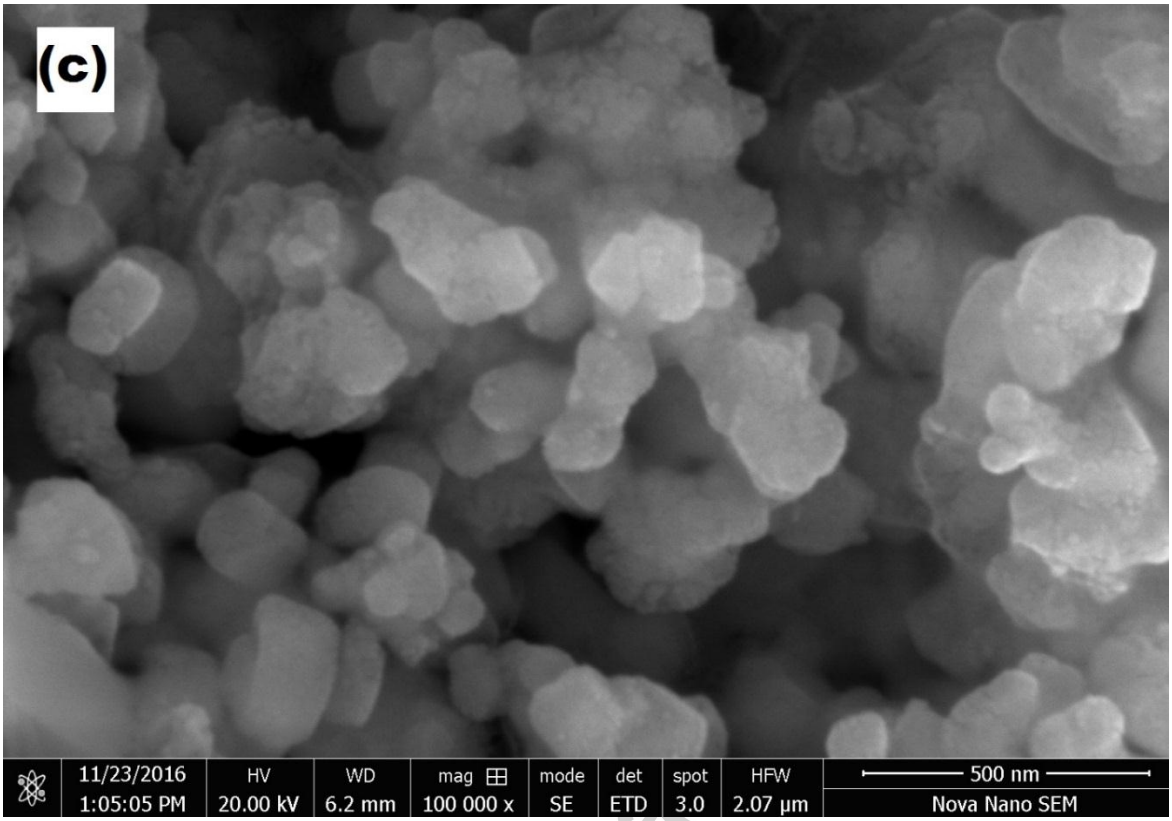

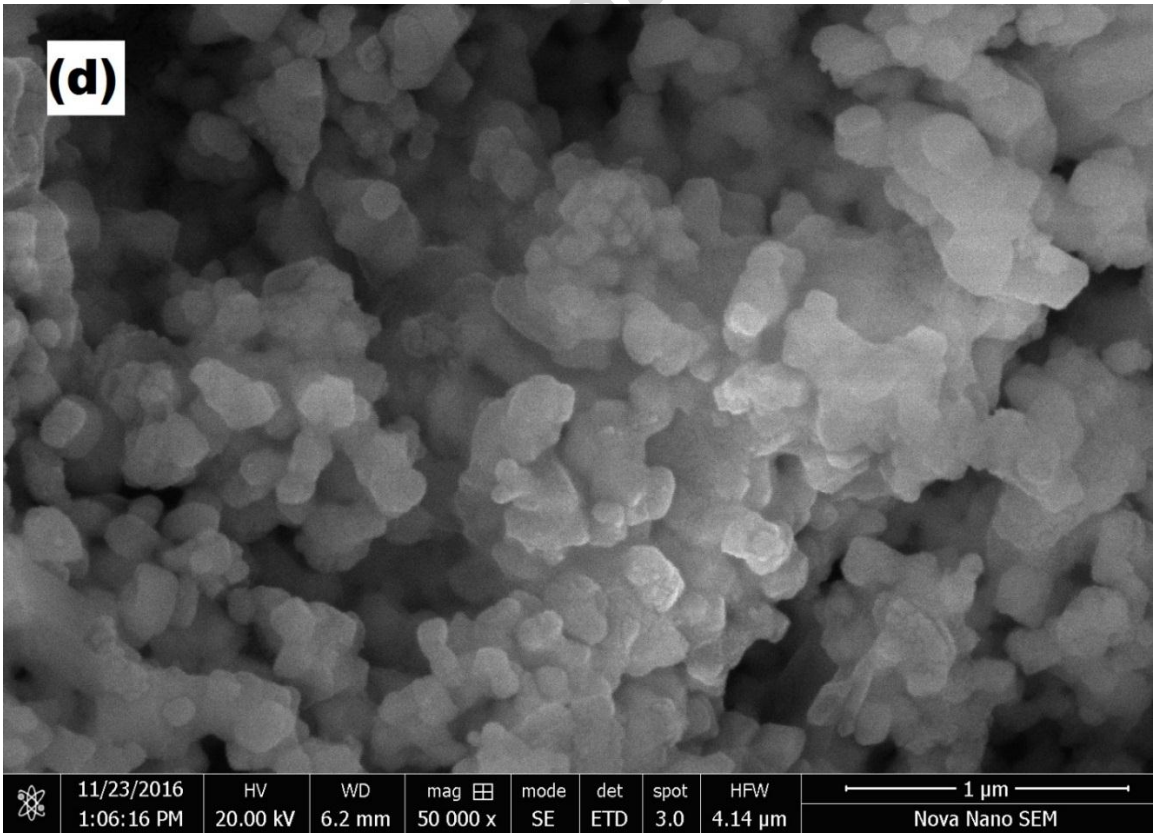

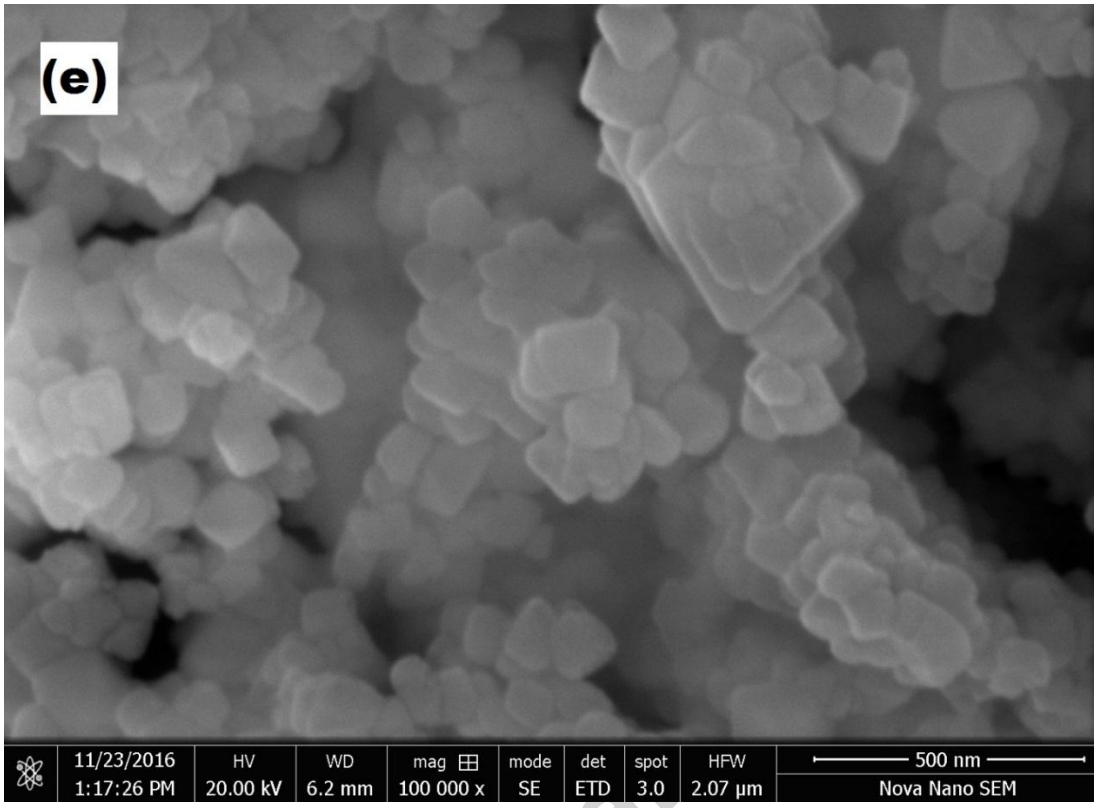

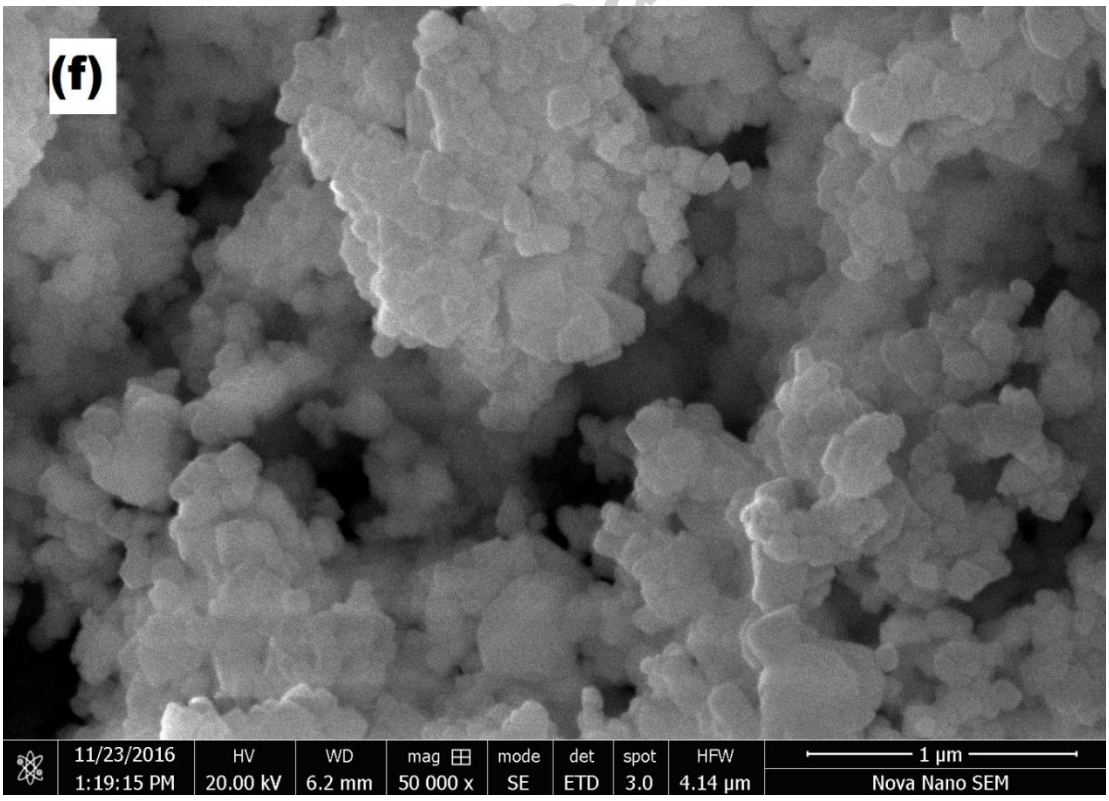

Figure 2: SEM images (a, b) $La_{0.2}Ce_{0.8}O_{2-\delta}$ (LDC), (c, d) $Zr_{0.2}Ce_{0.8}O_{2-\delta}$ (ZDC) and (e, f)

$Zr_{0.2}La_{0.2}Ce_{0.6}O_{2-\delta}$ (ZLDC).

Thermal Characterization

The thermogravimetric analysis (TGA) curves of these ceria doped electrolytes ($La_{0.2}Ce_{0.8}O_{2-\delta}$ (LDC), $Zr_{0.2}Ce_{0.8}O_{2-\delta}$ (ZDC) and $Zr_{0.2}La_{0.2}Ce_{0.6}O_{2-\delta}$ (ZLDC) are shown in Figure 3. The TGA curves explicate that there is no significant weight loss of these electrolytes with increase in temperature. As this loss is not more than 1% of the initial weight this confirms their excellent thermal stability. In region I (temp < 120 °C), there is slight weight loss for sample LDC, but quite prominent weight drop is noticed for ZDC and ZLDC which is specific to evaporation or solvent desorption. In region II (temp from 120 °C to 450 °C), there is a slight weight loss for LDC but gradual loss for other electrolytes has been observed which is due to the loss of volatilization products or thermo-oxidative decomposition reactions. Upon further increase in temperature above 450 °C (region III), the weight loss for ZDC and ZLDC is the same as in region II which could be ascribed to crystallization since the formation of crystallites attributes to weight loss during the process of crystallization from the amorphous phase. In region IV, further weight loss is observed for all samples, but no abrupt drop is seen. Weight loss for electrolyte LDC, at high temperature, is quite small compared to the other samples, which shows that it is more thermally stable.

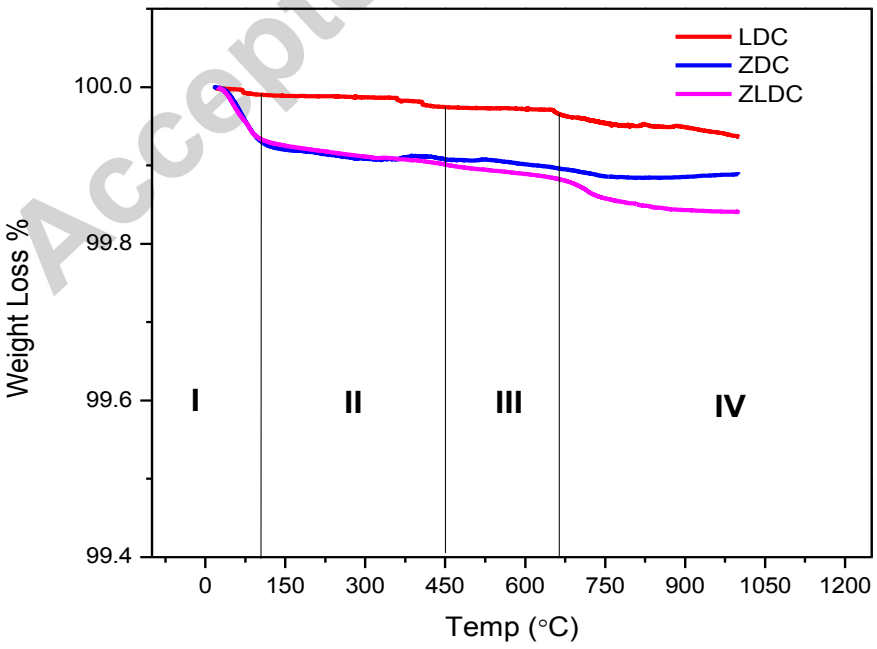

Figure 3: TGA curve of $La_{0.2}Ce_{0.8}O_{2-\delta}$ (LDC), $Zr_{0.2}Ce_{0.8}O_{2-\delta}$ (ZDC) and $Zr_{0.2}La_{0.2}Ce_{0.6}O_{2-\delta}$ (ZLDC).

Dilatometric Analysis

Thermal expansion of electrolyte materials plays a significant role in many SOFC applications. The TEC of the electrolyte must match well with that of the electrodes (anode/cathode) to avoid micro-cracks/internal stress developing in adjoining SOFC components at operating temperature [39]. The thermal expansion (dL/L_o) characteristics of the samples $La_{0.2}Ce_{0.8}O_{2-\delta}$ (LDC), $Zr_{0.2}Ce_{0.8}O_{2-\delta}$ (ZDC) and $Zr_{0.2}La_{0.2}Ce_{0.6}O_{2-\delta}$ (ZLDC) were measured from room temperature (RT) to 1450 °C and are represented in Figure 4. It shows that samples expand linearly with temperature from 100 ˚C to 1150 ˚C but expansion for LDC and ZDC is more linear than for ZLDC. Linear thermal expansion coefficients (TECs) of these samples were calculated from equation (ii) and are listed in Table 2. With the increase in temperature from RT to 1450 °C, variation in thermal expansion in the lattice is observed due to the formation of oxygen vacancies or loss of oxygen in differently doped ceria electrolytes. From Table 2, the values of TECs for LDC and ZDC in the temperature range from 150 to 1000 °C are 11.3×10^{-6} °C^{-1} and 12.2×10^{-6} °C^{-1} respectively. TEC for LDC and ZDC matches pretty well with the TEC of ceria (CeO_2) and doped ceria electrolytes as reported previously [4, 36, 40-46]. The TEC of ZLDC is 15.3×10^{-6} °C^{-1} in the temperature range 150 to 300 °C, which is close to the values reported as given in table 2. Hence, with further increase in temperature (>1170 °C), the TEC of ZLDC becomes negative as indicated in Figure 4(c) due to contraction of material upon further heating. TECs "α" of all samples tend to increase with increasing temperature up to 1170 °C, which is due to the increase of content of oxygen. This increase in the oxygen vacancy leads to the weakening of the binding energy, which is responsible for the increase in the value of TEC. The thermal expansion behavior of ZLDC is different from the other two electrolytes at higher temper > 1150 °C which is because of co-doping of both La (1.061 Å) and Zr (0.72 Å) of different ionic radii. The values of TECs for LDC, ZDC and ZLDC from RT to 1450 °C are as follows: 9.1×10^{-6} °C^{-1}, 8.6×10^{-6} °C^{-1}, and -15.6 × 10-6 ° C^{-1}, respectively.

Furthermore, these doped/co-doped ceria electrolytes showed a good compatibility with more commonly used anodes; NiO and YSZ in different temperature range as reported in different studies [47-51]. As Gillam *et al*. reported, the TEC for NiO is 13.9×10^{-6} °C^{-1} in the temperature

range 160 to 1300 °C [48], which is in good concurrence to our TECs as mentioned in Table 2. Similarly, these TECs for LDC, ZDC and ZLDC are in good agreement with NiO (14.1×10^{-6} °C^{-1}) and YSZ (10.3×10^{-6} °C^{-1}) as reported by Masashi *et al.* [50]. The calculated TECs of prepared electrolytes also match well with the cathode material $La_{0.65}Sr_{0.3}MnO_{3-\delta}$ (12.3×10^{-6} °C^{-1}) [46] and cathode composite BSCN- 40GDC (13.5×10^{-6} °C^{-1}) reported by Leilei *et al.* [35]. The harmony between the TEC of electrolyte materials with electrodes results in reducing the thermal stress in SOFC and good long-term thermal stability.

Table 2: TEC of different electrolytes used for SOFC

Temperature (°C)	**TEC α (×10^{-6} °C^{-1})**			**Reference**
	$La_{0.2}Ce_{0.8}O_{2-\delta}$ *(LDC)*	$Zr_{0.2}Ce_{0.8}O_{2-\delta}$ *(ZDC)*	$Zr_{0.2}La_{0.2}Ce_{0.6}O_{2-\delta}$ *(ZLDC)*	Prepared samples
150 – 1000	11.3	12.2	4.5	
150 – 1300	13.4	13.6	15.3	
	CeO_2	$Ce_{0.8}La_{0.2}O_{1.9}$	$Ce_{0.8}Sm_{0.2}O_{1.9}$	Literature
25 - 1000	12	12	12	[40]
1000	13.3	13.2	13.4	[40]
	$Ce_{0.8}Gd_{0.2}O_{1.9}$	$Ce_{0.9}Sr_{0.1}O_{1.9}$	$Zr_{0.85}Y_{0.15}O_{1.93}$ *(8YSZ)*	
30 - 800	12.5	12.8	10.5	[44]
30 - 1000	12.7	13.1	10.9	[44]

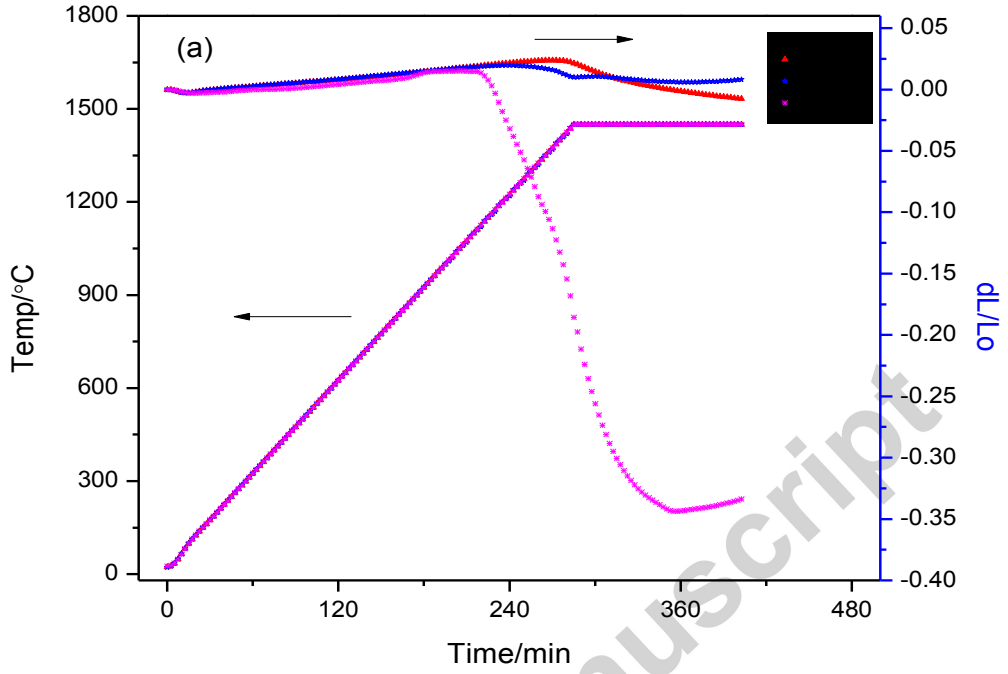

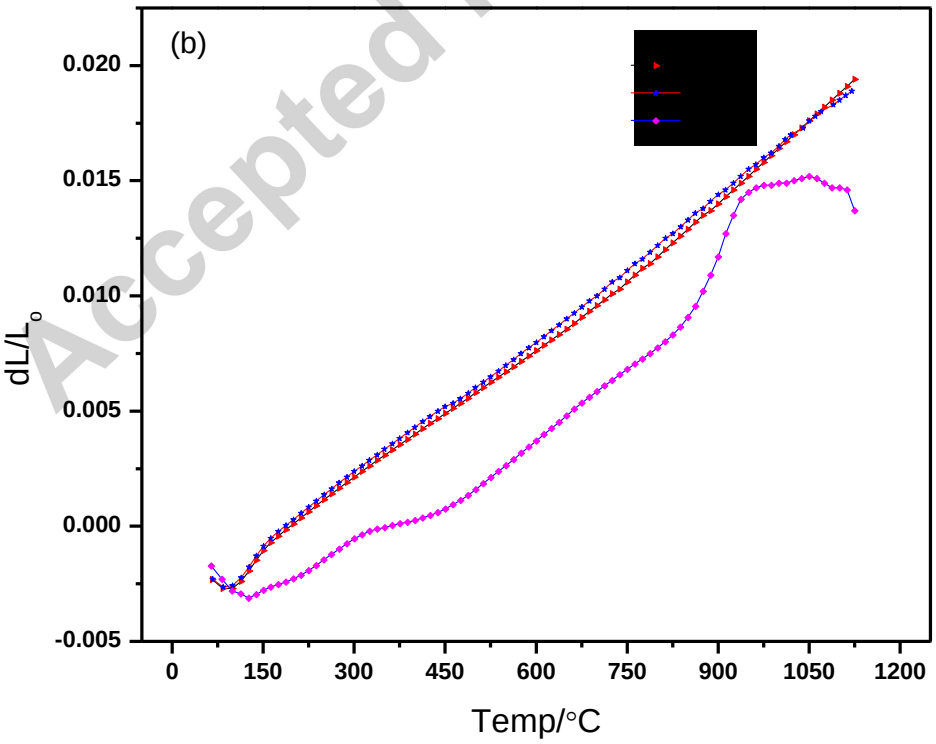

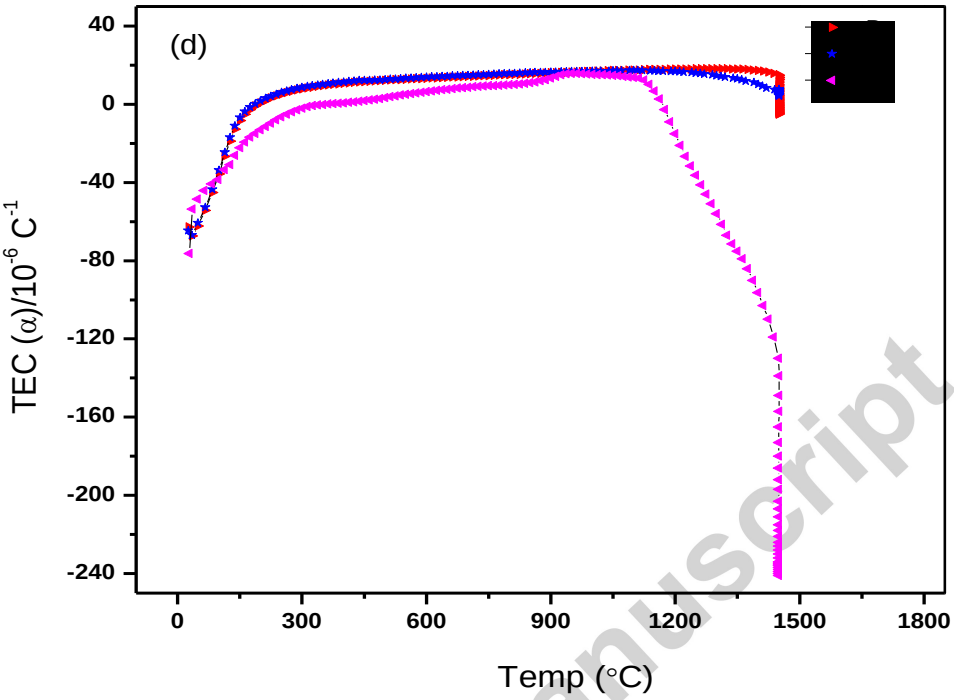

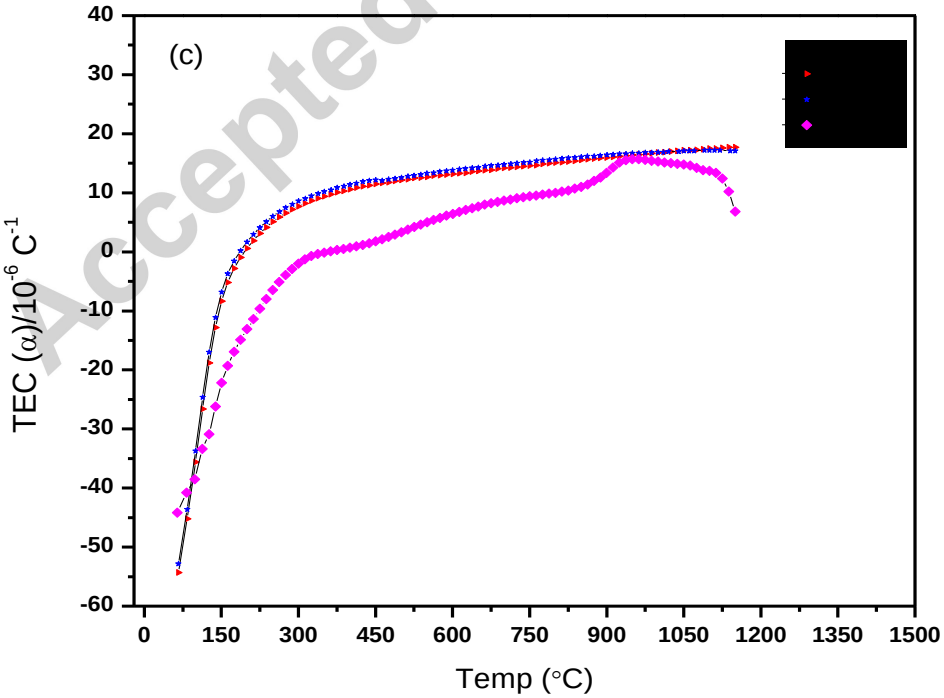

Figure 4: (a, b) Thermal expansion from RT to 1450 °C /60 to 1150 °C and (c,d) TEC curves of $La_{0.2}Ce_{0.8}O_{2-\delta}$ (LDC), $Zr_{0.2}Ce_{0.8}O_{2-\delta}$ (ZDC) and $Zr_{0.2}La_{0.2}Ce_{0.6}O_{2-\delta}$ (ZLDC) from temp RT to 1450 °C/60 to 1150°C.

DC Conductivity

The Arrhenius plots for the conductivity of $La_{0.2}Ce_{0.8}O$ (LDC), $Zr_{0.2}Ce_{0.8}O_{2-\delta}$ (ZDC) and $Zr_{0.2}La_{0.2}Ce_{0.6}O_{2-\delta}$ (ZLDC) are represented in Figure 5. This shows the dependence of Ln(σT) versus 10^3/T, which is nearly linear. The ionic conductivity (bulk) is the sum of grain interior and grain boundary contribution [52]. The ionic conductivity of pure ceria is $0.24\pm0.02 \times 10^{-3}$ S.cm^{-1} at a temperature of 800 °C which is low at high temperature. The ionic conductivity can be enhanced significantly in rare-earth-doped-ceria ceramics by incorporating the increase of oxygen vacancy.

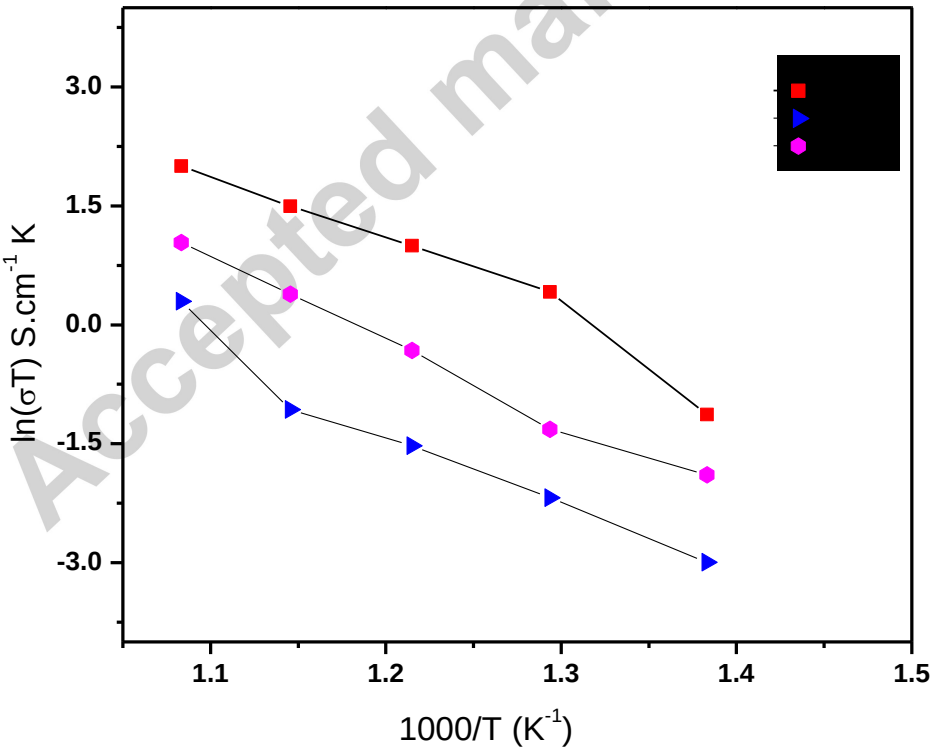

Figure 5: Arrhenius plot for ionic conductivity of $La_{0.2}Ce_{0.8}O_{2-\delta}$ (LDC), $Zr_{0.2}Ce_{0.8}O_{2-\delta}$ (ZDC) and $Zr_{0.2}La_{0.2}Ce_{0.6}O_{2-\delta}$ (ZLDC).

Here, the ionic conductivity of CeO_2 with dopants La^{3+} and $Zr^{4+}$is reported. It has been observed that with an increase in temperature, ionic conductivity in these samples increased because at high temperature, oxide ion mobility also increases. Using the Arrhenius equation, the activation energy for the total conductivity was calculated by fitting the data of conductivity (σ) from the slopes in the temperature range 450 to 650 °C.

$$\sigma = \frac{A}{T} \exp(\frac{-Ea}{kT}) \qquad \text{(iii)}$$

Where "E_a" is the activation energy for the migration of oxygen ions, "k" is the Boltzman constant, "T" is the temperature in Kelvin, and "A" is the pre-exponential factor.

The ionic conductivities at 650°C, are in the order of $La_{0.2}Ce_{0.8}O_{2-\delta}$ (0.81×10^{-2} S.cm^{-1}) > $Zr_{0.2}La_{0.2}Ce_{0.6}O_{2-\delta}$ (0.32×10^{-2} S.cm^{-1}) > $Zr_{0.2}Ce_{0.8}O_{2-\delta}$ (0.15×10^{-2} S.cm^{-1}) with their corresponding activation energies 0.86, 0.87 and 0.88 eV, respectively. The ionic conductivities of $La_{0.2}Ce_{0.8}O_{2-\delta}$ at 500 °C and 600 °C are 0.195×10^{-2} S.cm^{-1} and 0.51×10^{-2} S.cm^{-1}, respectively, which are higher than the values reported by Nandini *et al.* [31] for $Ce_{0.85}La_{0.15}O_{1.925}$ (0.02×10^{-2} S.cm^{-1} at 500 °C and 0.094×10^{-2} S.cm^{-1}). Furthermore, the activation energy 0.86 eV for LDC in our study is less than 0.97 eV as reported in [31]. The increase in bulk conductivity leads to the enhancement of oxygen vacancies, as a result ordering of these oxygen vacancies is suppressed which ascribes to a decrease in activation energy for the diffusion of oxygen ions [53]. Ionic conductivity of $La_{0.2}Ce_{0.8}O$ (LDC) at 650°C in this study is higher than $Ce_{0.8}Er_{0.2-x}La_xO_{1.9}$ (for composition x=0.06) as represented by Qian *et al.* [54]

Generally, total conductivity of ceria doped with rare-earth metal ions is the sum of both ionic and electronic conductivity. However, the contribution of electronic conductivity in air for ceria based materials is negligible ≈ 10^{-6} S.cm^{-1} as compared to ionic conductivity ≈ 10^{-2} S.cm^{-1} for temperatures less than 800˚C [20, 55]. As in our study the temperature range is 450 to 650^{o}C, therefore, electronic conductivity can be neglected, and the apparent conductivity is due to the contribution of only ions.

AC Electrochemical Impedance Spectroscopy

AC EIS is a powerful tool to investigate the electrical response of an electrolyte and hence to elucidate the total ionic conductivity from the contribution of grain interior, grain boundary, and electrode. The impedance spectra in the form of a Nyquist plot of doped/co-doped ceria

electrolytes (LDC, ZDC and ZLDC) are shown in Figure 6(a-c), in the temperature range 450 to 650˚C. In general, the Nyquist plot at low temperature gives two semi-circles and one incomplete semi-circle/tail which is specific to the frequency range of the instrument and applied temperatures [21]. The first semi half circle at high frequency (Capacitance C □ 10^{-12}-10^{-10}F) corresponds to the resistance of the grain bulk (R_{gi}), the next semi-circle at intermediate frequency (C □ 10^{-9}-10^{-7} F) represents blocking of oxygen vacancies at the grain boundary (R_{gb}), and the incomplete arc at low frequency (C <10^{-7} F) corresponds to electrode resistance (R_{el}). However, from impedance plots of electrolytes as shown in Figure 6(a-c) not all the arcs are observed due to our high frequency limitation. Instead of two semi circles, one semi-circle/arc which corresponds to grain boundary resistance, and some part of a depressed tail that corresponds to electrolyte-electrode interface reactions are represented in the Nyquist plot. The size of impedance arcs decreases with the increase of temperature for electrolytes LDC, ZDC and ZLDC, but impedance response of LDC is smoother than the others. As the temperature increases, the arcs shift toward higher frequency due to the relaxation frequencies of different polarization processes which leads to the disappearance of independent arcs due to a limited frequency range [56]. The impedance arc for LDC is quite prominent at lower temperature compared to ZDC and ZLDC as plotted in Figure 6(a-c), which corresponds to the grain boundary capacitance in the range of nF. The capacitance is obtained from the relation [56]:

$$C = \frac{1}{2\pi f R} \qquad \text{(iv)}$$

Where “f” is the applied frequency at the arc/semi-circle maximum and “R” is the resistance which is obtained from the arc intercept on the Z real axis. Similarly, capacitance determined from arcs for ZDC and ZLDC also lies in the nF range which is associated with the grain boundary resistance. Hence, some part of tail for ZDC and ZLDC is displayed on impedance spectra and capacitance for these depressed tails for all samples lies in the range 10^{-4}-10^{-3}F, which corresponds to electrolyte/electrode interface polarization.

The equivalent circuits used for fitting the experimental data consisted of (LR QR QR), which is shown inset of the figures, where L is the inductance which can be attributed to the connecting wires, R is the resistance of the material, and Q is a constant phase element.

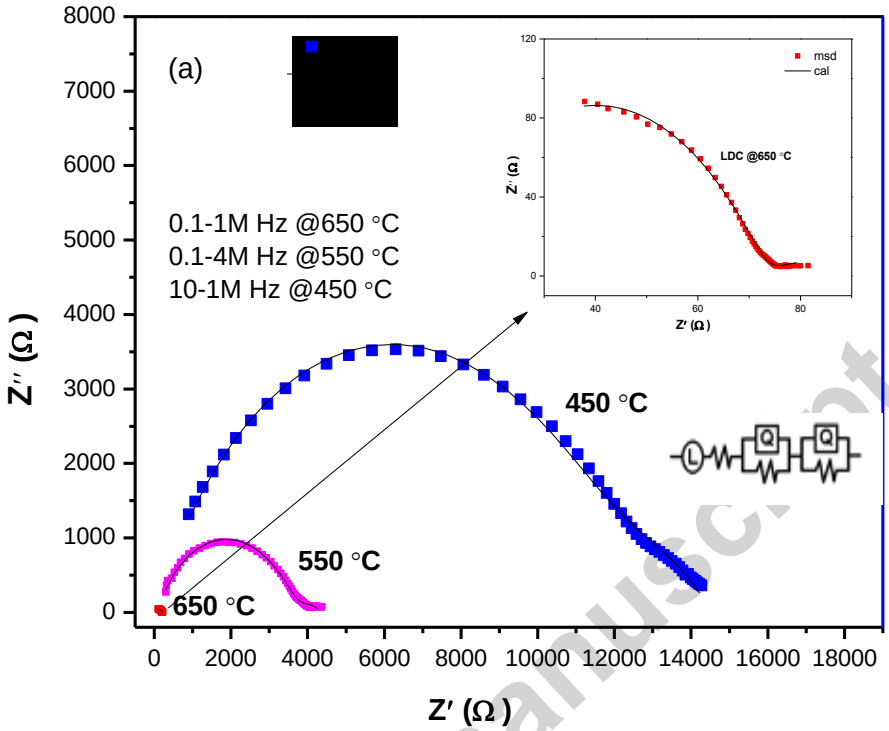

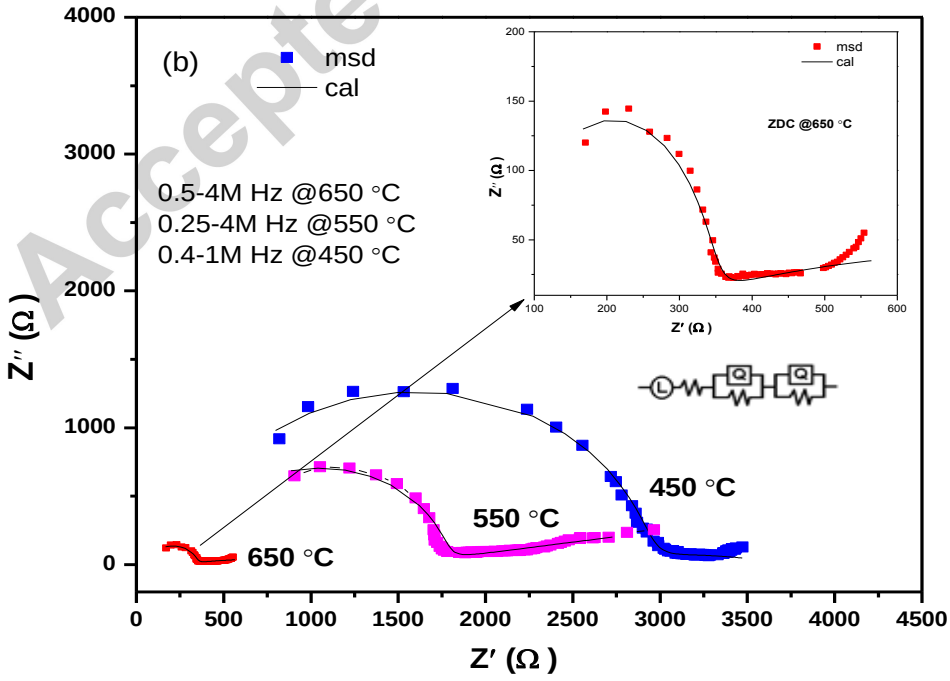

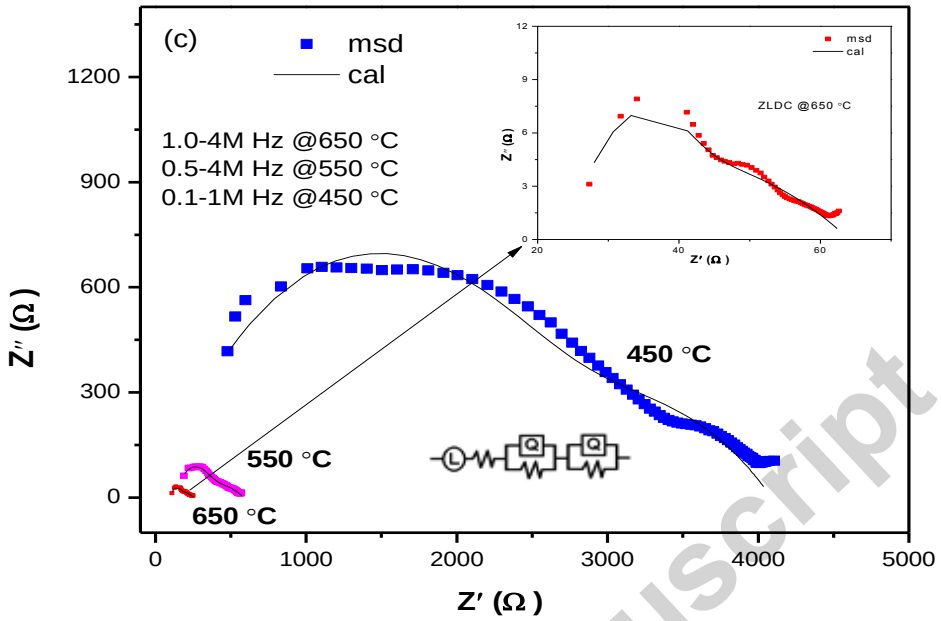

Figure 6(a-c): Impedance plots for $La_{0.2}Ce_{0.8}O_{2-\delta}$ (LDC), $Zr_{0.2}Ce_{0.8}O_{2-\delta}$ (ZDC) and $Zr_{0.2}La_{0.2}Ce_{0.6}O_{2-\delta}$ (ZLDC).

Conclusion:

Doped and co-doped ceria composites have been presented as an efficient electrolyte candidate for the intermediate temperature solid oxide fuel cell (IT-SOFC). Nanocomposites: $La_{0.2}Ce_{0.8}O_{2-\delta}$ (LDC), $Zr_{0.2}Ce_{0.8}O_{2-\delta}$ (ZDC), and $Zr_{0.2}La_{0.2}Ce_{0.6}O_{2-\delta}$ (ZLDC) have been successfully synthesized via a co-precipitation technique to study the doping effect of La^{3+} and Zr^{4+} with ceria. The obtained powders have cubic fluorite structure with crystallite size in the nanometric range (20 to 45 nm) from XRD analysis. TGA and dilatometry have been carried out to investigate the effect of temperature on sample weight and length, respectively. All samples have shown excellent thermal stability, as no significant weight loss (less than 1%) was observed in the temperature range RT to 1000˚C. Thermal expansion coefficients (TECs) were calculated as follows: 13.4×10^{-6} °C^{-1}, 13.6×10^{-6} °C^{-1} and 15.3×10^{-6} °C^{-1} for LDC, ZDC and ZLDC, respectively, in the temperature range 150 to 1150°C. Our reported TECs have shown good concurrence to most commonly used electrolytes and anode/cathode. Ionic conductivity has been studied for doped ceria electrolytes in the temperature range 450 to 650˚C and are ranked as follows: $La_{0.2}Ce_{0.8}O_{2-\delta}$ (LDC) > $Zr_{0.2}La_{0.2}Ce_{0.6}O_{2-\delta}$ (ZDC) > $Zr_{0.2}Ce_{0.8}O_{2-\delta}$ (ZLDC) with their corresponding activation

energies 0.86, 0.87 and 0.88 eV. The results revealed that $La_{0.2}Ce_{0.8}O_{2-\delta}$ shows the highest ionic conductivity of 0.81×10^{-2} S.cm^{-1} at 650˚C compared to other ceria doped electrolytes.

Acknowledgements

The authors gratefully acknowledge the

IRSIP/HEC, Govt. of Pakistan scholarship to visit the fuel cell labs at the School of Chemical Engineering, University of Birmingham, UK.

References

[1] S.C.Singhal, K.Kendall (eds.): High-temperature Solid Oxide Fuel Cells: Fundamentals, Design and Applications. Elsevier, 2003.

[2] M.D. Mat, X. Liu, Z. Zhu, B. Zhu, Development of cathodes for methanol and ethanol fuelled low temperature (300–600 C) solid oxide fuel cells, International journal of hydrogen energy 32 (7) (2007) 796-801.

[3] S. Park, J.M. Vohs, R.J. Gorte, Direct oxidation of hydrocarbons in a solid-oxide fuel cell

Nature 404 (2000) 265-267.

[4] Y. Mizutani, M. Tamura, M. Kawai, O. Yamamoto, Development of high-performance electrolyte in SOFC, Solid State Ionics 72 (1994) 271− 275.

[5] H.A. Taroco, J.A.F. Santos,R.Z. Domingues, T. Matencio, Ceramic Materials for Solid Oxide Fuel Cells, Advances in Ceramics - Synthesis and Characterization, Processing and Specific Applications, Prof. Costas Sikalidis (Ed.), InTech (2011). ISBN: 978-953-307-505-1.

[6] M.C. Brant, T. Matencio, L. Dessemond, R.Z. Domingues, Electrical degradation of porous and dense LSM/YSZ interface, Solid State Ionics 177 (9-10) (2006) 915-921.

[7] K. Nomura, Y. Mizutani, M. Kawai, Y. Nakamura, O. Yamamoto, Aging and Raman scattering study of scandia and yttria doped zirconia, Solid State Ionics 132 (3–4) (2000) 235–239.

[8] C. Haering, A. Roosen, H. Schichl, M. Schnöller, Degradation of the electrical conductivity in stabilised zirconia system: Part II: scandia-stabilised zirconia, Solid State Ionics 176 (3–4) (2005) 261–268.

[9] O. Yamamoto, Y. Arati, Y. Takeda, N. Imanishi, Y. Mizutani, M. Kawai, Y. Nakamura, Electrical conductivity of stabilized zirconia with ytterbia and scandia, Solid State Ionics 79

(1995) 137–142.

[10] S. Omar, A. Belda, A. Escardino, N. Bonanos, Ionic conductivity ageing investigation of 1Ce10ScSZ in different partial pressures of oxygen, Solid State Ionics 184 (1) (2011) 2–5.

[11] M. Hirano, T. Oda , K. Ukai , Y. Mizutani, Effect of Bi_2O_3 additives in Sc stabilized zirconia electrolyte on a stability of crystal phase and electrolyte properties, Solid State Ionics 158 (3) (2003) 215–223.

[12] C. Varanasi, C. Juneja, C. Chen, B. Kumar, Electrical conductivity enhancement in heterogeneously doped scandia-stabilize zirconia, Journal of Power Sources 147 (1–2) (2005) 128–135.

[13] F. Yuan, J. Wang, H. Miao, C. Guo, W.G. Wang, Investigation of the crystal structure and ionic conductivity in the ternary system $(Yb_2O_3)_x$–$(Sc_2O_3)_{(0.11-x)}$–$(ZrO_2)_{0.89}$ (x = 0−0.11), Journal of Alloys and Compounds 549 (2013) 200–205.

[14] Z. Lei, Q. Zhu, Phase transformation and low temperature sintering of manganese oxide and scandia co-doped zirconia, Materials Letters 61 (6) (2007) 1311–1314.

[15] Y. Arachi, T. Asai, O. Yamamoto, Y. Takeda, N. Imanishi, K. Kawate, C. Tamakoshi, Electrical conductivity of ZrO2–Sc2O3 doped with HfO2, CeO2, and Ga2O3, Journal of the Electrochemical Society 148 (5) (2001) A520–A523.

[16] A.S. Nesaraj, Recent developments in solid oxide fuel cell technology – a review, Journal of Scientific and Industrial Research, 69 (3) (2010) 169-176.

[17] B. Zhu, Functional ceria–salt-composite materials for advanced ITSOFC applications J. Power Sources 114 (1) (2003) 1-9.

[18] M. Dudek, Composite Oxide Electrolytes for Electrochemical Devices, Advances in Materials Science 8 (1) (2008) 15-30

[19] M.L. Faro, D. La Rosa, V. Antonucci, A.S. Arico, Intermediate temperature solid oxide fuel cell electrolytes, Journal of the Indian Institute of Science 89 (4) (2009) 363-380.

[20] H. Inaba, H. Tagawa, Ceria-based solid electrolytes, Solid State Ionics 83 (1-2) (1996) 1-16.

[21] S. Kuharuangrong, Ionic conductivity of Sm, Gd, Dy and Er-doped ceria, J. Power Sources 171 (2) (2007) 506-510.

[22] J.W. Fergus, Electrolytes for solid oxide fuel cells, J. Power Sources 162 (1) (2006) 30-40.

[23] A. Gondolini, E. Mercadelli, A. Sanson, S. Albonetti, L. Doubova, S. Boldrini, Microwave-assisted synthesis of gadolinia-doped ceria powders for solid oxide fuel cells, Ceramics International 37(4) (2011) 1423-1426.

[24] M. Dudek, Ceramic Electrolytes in the CeO_2-Gd_2O_3-SrO System – Preparation, Properties and Application for Solid Oxide Fuel Cells, Int. J. Electrochem. Sci., 7 (2012) 2874-2889.

[25] J.W. Fergus, R. Hui, X. Li, D.P. Wilkinson, J. Zhang, Solid oxide fuel cells: materials properties and performance, CRC Press London New York, USA eds., 2016.

[26] M. Kahlaoui, S. Chefi, A. Inoubli, A. Madani, C. Chefi, Synthesis and electrical properties of co-doping with La^{3+}, Nd^{3+}, Y^{3+} and Eu^{3+} citric acid-nitrate prepared samarium-doped ceria ceramics, Ceram. Int. 39 (4) (2013) 3873–3879.

[27] A. Rafique, R. Raza, N. Akram, M.K. Ullah, A. Ali, M. Irshad, K. Siraj, M.A. Khan, B. Zhu, R. Dawson, Significance enhancement in the conductivity of core shell nanocomposite electrolytes, RSC Advances 5 (105) (2015) 86322-86329.

[28] Y. Zheng, L. Wu, H. Gu, L. Gao, H. Chen, L. Guo. The effect of Sr on the properties of Y-doped ceria electrolyte for IT-SOFCs, J. Alloys Compd. 486(1) (2009) 586-589.

[29] B. Li, X. Wei, W. Pan, Improved electrical conductivity of $Ce_{0.9}Gd_{0.1}O_{1.95}$ and $Ce_{0.9}Sm_{0.1}O_{1.95}$ by co-doping, Int. J. Hydrogen Energy 35(7) (2010) 3018-3022.

[30] Y.P. Fu, S.B. Wen, C.H. Lu, Preparation and Characterization of Samaria-Doped Ceria Electrolyte Materials for Solid Oxide Fuel Cells, Journal of the American Ceramic Society, 91(1) (2008) 127-131.

[31] N. Jaiswal, S. Upadhyay, D. Kumar, O. Parkash, Ionic conductivity investigation in lanthanum (La) and strontium (Sr) co-doped ceria system, Journal of Power Sources 222 (2013) 230-236.

[32] M. Dudek, Ceramic oxide electrolytes based on CeO2—Preparation, properties and possibility of application to electrochemical devices. J. Eur Ceram Soc 28 (5) (2008) 965–971.

[33] N. Mahato, A. Banerjee, A. Gupta, S. Omar, K. Balani, Progress in material selection for solid oxide fuel cell technology: A review, Prog Mater Sci 72 (2015) 141–337.

[34] H. Hayashi, M. Kanoh, C.J. Quan, H. Inaba, S. Wang, M. Dokiya, H. Tagawa, Thermal expansion of Gd-doped ceria and reduced ceria, Solid State Ionics 132 (3) (2000) 227 –233.

[35] L. Zhang, M. Liu, J. Huang, Z. Song, Y. Fu, Y. Chang, C. Li, T. He, Improved thermal expansion and electrochemical performances of $Ba_{0.6}Sr_{0.4}Co_{0.9}Nb_{0.1}O_{3-\delta}$–$Gd_{0.1}Ce_{0.9}O_{1.95}$ composite cathodes for IT-SOFCs, Int. J. Hyd. Energy 39 (15) (2014) 7972–7979.

[36] K. Venkataramana, C. Madhusudan, C. Madhuri, C.V. Reddy, Synthesis, characterization and thermal expansion of $Ce_{0.8-x}Sm_{0.2}Zr_xO_{2-\delta}$ Solid electrolytes for IT-SOFC applications, Materials Today: Proceedings 3 (10) (2016) 3908–3913.

[37] R. Raza, X. Wang, Y. Ma, B. Zhu, Study on calcium and samarium co-doped ceria based nanocomposite electrolytes, Journal of Power Sources 195 (19) (2010) 6491–6495.

[38] S. Omar, E.D. Wachsman, J.L. Jones, J.C. Nino, Crystal Structure–Ionic Conductivity Relationships in Doped Ceria Systems, J. Am. Ceram. Soc. 92 (11) (2009) 2674–2681.

[39] S. Ramesh, V. Prashanth Kumar, P. Kistaiah and C. Vishnuvardhan Reddy, Preparation, characterization and thermo electrical properties of co-doped $Ce_{0.8-x}Sm_{0.2}Ca_xO_{2-\delta}$ materials, Solid State Ionics 181 (1) (2010) 86–91.

[40] S. Sameshima, M. Kawaminami, Y. Hirata, Thermal expansion of Rare-Earth-doped Ceria Ceramics, Journal of the Ceramic Society of Japan 110(7) 597-600 (2002).

[41] R.L. Wilfong, L.P. Domingues, L. R. Furlong, J. A. Finlayson, Thermal Expansion of the Oxides of Yttrium, Cerium, Samarium, Europium and Dysprosium, Bureau of Mines. College Park Metallurgy Research Center, Md., No. BM-RI-6180 (1962).

[42] J. R. Sims Jr, R. N. Blumenthal, Defect structure investigation of nonstoichiometric cerium dioxide: I, High temperature X-ray lattice parameter measurements, High Temp. Sci. 8 (2) 99 (1976).

[43] S. Stecura, W.J. Campbell, Thermal Expansion and Phase Inversion of Rare Earth Oxides, Bureau of Mines, College Park Metallurgy Research Center, Md. No. BM-RI-5847 (1960).

[44] F. Tietz, G. Stochniol, A. Naoumidis, Proc. 5th Eur. Conf. on Advanced Materials, Processes and Applications (Euromat '97), eds.: L. A. J. L. Sarton, H. B. Zeedijk, Netherlands Society for Materials Science 2, (1997), 271.

[45] R. Maenner, E. Ivers-Tiff~e, W. Wersing, W. Kleinlien, Proc. 2nd Eur. Ceram. Soc. Conf. (Euro-Ceramics II), eds.: G. Ziegler, H. Hausner, Deutsche Keramische Gesellschaft (1991), p. 2085.

[46] F. Tietz, Thermal Expansion of SOFC Materials, Ionics 5(1) (1999) 129-139.

[47] R. L. Clendenen, H. G. Drickamer, Lattice parameters of nine oxides and sulfides as a function of pressure, J. Chem. Phys. 44 (11) (1966) 4223-4228.

[48] E. Gillam, J.P. Holden, Structure of nickel oxide containing alumina, J. Am. Ceram. Soc. 46 (12) (1963) 601-604.

[49] L.C. Bertel, B. Morosin, Exchange striction in NiO, Phys. Rev. B 3 (3) (1971) 1039.

[50] M. Mori, T. Yamamoto, H. Itoh, H. Inaba, H. Tagawa, Thermal Expansion of Nickel-Zirconia Anodes in Solid Oxide Fuel Cells during Fabrication and Operation, Journal of the Electrochemical Society 145 (4) (1998) 1374-1381.

[51] Y.S. Touloukian, R.K. Kirby, E.R. Taylor, T.Y.R. Lee, Thermophysical Properties of Matter, The TPRC Data Series Vol. 13, Thermal Expansion, Nonmetallic Solids (1977), 1689

[52] C. Tian, S.W. Chan, Ionic conductivities, sintering temperatures and microstructures of bulk ceramic CeO_2 doped with Y_2O_3, Sol Stat Ionics 134 (1) (2000) 89–102.

[53] H. Yamamura, E. Katoh, M. Ichikawa, K. Kakinuma, T. Mori, H. Haneda, Multiple doping effect on the electrical conductivity in the (Ce (1-xy) La (x) My) O2-delta (M=Ca, Sr) system. Electrochemistry 68 (6) (2000) 455–459.

[54] Q. Hu, F. Yang, H. Fang, C. Zhao, The Preparation and Electrical Properties of La Doped $Er_{0.2}Ce_{0.8}O_{1.9}$ Based Solid Electrolyte, Int. J. Electrochem. Sci. 12 (8) (2017) 7411–7425.

[55] B.C.H. Steele, Appraisal of $Ce_{1-y}Gd_yO_{2-y/2}$ electrolytes for IT-SOFC operation at 500 ˚C, Solid state ionics 129 (1) (2000) 95–110.

[56] N. Jaiswal, D. Kumar, S. Upadhyay, O. Parkash, Preparation and characterization of $Ce_{0.85}La_{0.15-x}Sr_xO_{\{2-(0.075+x/2)\}}$ solid electrolytes for intermediate temperature solid oxide fuel cells, Ionics 21 (2) (2015) 497-505.